Optimal Engine Operation by Shift Speed Control of a CVT

Heera Lee
Graduate Student, School of Mechanical Engineering, Sungkyunkwan University, Kyunggido 440-746, Korea
Hyunsoo Kim*
Professor, School of Mechanical Engineering, Sungkyunkwan University, Kyunggido 440-746, Korea

In this paper, an algorithm to increase the shift speed is suggested by increasing the line pressure for a metal belt CVT. In order to control the shift speed, an algorithm to calculate the target shift speed is presented from the modified CVT shift dynamics. In applying the shift speed control algorithm, a criterion is proposed to prevent the excessive hydraulic loss due to the increased line pressure. Simulations are performed based on the dynamic models of the hydraulic control valves, powertrain and the vehicle. It is found from the simulation results that performance of the engine operation can be improved by the faster shift speed, which results in the improved fuel economy by 2% compared with that of the conventional electronic control CVT in spite of the increased hydraulic loss due to the increased line pressure.

Key Words: CVT(Continuously Variable Transmission), Line Pressure, Shift Speed

1. Introduction

In a metal belt CVT, the secondary pressure, in other words, the line pressure control is performed to supply an optimal belt clamping force for a given torque and speed ratio. An excessive line pressure causes a hydraulic power loss as well as a short fatigue life of the belt meanwhile an insufficient line pressure results in a slippage between the belt and the pulley. On the other hand, the primary pressure control is required to provide an optimal speed ratio, which is directly related with the fuel economy and driveability of the vehicle.

It is well known that the CVT has many advantages over 4-5 stepped automatic transmissions since the CVT is able to provide an optimal engine operation by changing the speed ratio in a continuous manner. However, a r -latively slow response of the speed ratio has been pointed out as one of the major drawbacks of the metal belt CVT. To shorten the response time of the CVT powertran, torque assist of a flywheel was proposed with local controllers of the various process from pedal operation to vehicle speed (Serrarens and Veldpaus, 1999; Vroeman et al, 2001). For the CVT powertrain with the flywheel, a feedforward pressure control algorithm was suggested in controlling the speed ratio (Vroemen and Veldpaus, 1999; Vroeman, 2001). In this CVT hydraulic circuit, the primary pressure has a trouble following its setpoint, due to interaction with the secondary pressure. A model based control by a feedback linearization of the CVT system was performed (Lann, 1999) showing that the engine speed deviation from the optimal speed can be reduced by a faster shift speed. These models lacked dynamic model of the ratio and line pressure control valve which have nonlinear characteristics. To improve the driveability of a CVT powertrain, an integrated engine-CVT con-

* Corresponding Author,
E-mail: hskim@me.skku.ac.kr
TEL: +82-31-290-7473; **FAX**: +82-31-290-5849
Professor, School of Mechanical Engineering, Sungkyunkwan University, Kyunggido 440-746, Korea.
(Manuscript **Received** August 11, 2001; **Revised** April 9, 2002)

trol algorithm was proposed while achieving the engine operation near to the optimal operating line (OOL) during acceleration (Kim and Kim, 2000). To implement the algorithm, a throttle actuator and controlling system are required which give rise to an additional cost. In the previous study, Lee et al. (2000) showed experimentally that the improvement of the CVT shift speed can be obtained by increasing the line pressure and suggested a model based control algorithm based on the simplified dynamic models of the line pressure and the ratio control valve by considering nonlinear characteristics of the control valves.

In this study, an algorithm to obtain a faster shift speed is suggested for a metal belt CVT and it is shown that the improved fuel economy can be achieved by controlling the shift speed, which provides the improved engine operation on the OOL.

2. Shift Speed Control Algorithm

The CVT shift dynamics is represented as the following equation (T. Ide, 1996).

$$\frac{di}{dt}=\beta(i)\,\omega_p(P_p-P_p^*) \tag{1}$$

where di/dt is the shift speed, $\beta(i)$ is the coefficient which depends on the speed ratio i, ω_p is the primary speed, P_p is the applied primary pressure, P_p^* is the primary pressure at a steady state. Rearranging Eq. (1) gives,

$$\begin{aligned}\frac{di}{dt}&=\beta(i)\,\omega_p(P_p-P_p^*)\\&=\beta(i)\,\omega_p P_p\left(1-\frac{P_p^*}{P_p}\right)\\&=\beta(i)\,\omega_p\frac{F_p}{F_s}\frac{A_s}{A_p}P_s\left(1-\frac{P_p^*}{P_p}\right)\\&=\alpha(i)\,\omega_p P_s\left(1-\frac{P_p^*}{P_p}\right)\end{aligned} \tag{2}$$

where $\alpha(i)=\beta(i)F_pA_s/F_sA_p$, F and A denote the thrust and the actuator area, subscripts p and s denote the primary and secondary respectively. The thrust ratio F_p/F_s is known as a function of speed ratio i.

It is noted from Eq. (2) that the shift speed can be increased by increasing the line pressure P_s. Figure 1 shows a shift speed map for various line pressures when the upshift is carried out from a drive-off gear ratio, $i=2.48$. The shift speed map is constructed from the CVT shift dynamics, Eq. (2) at $\omega_p=2000$rpm. In calculating the shift speed, a safety factor 1.3 for the line pressure is used to guarantee the torque capacity of CVT. When the line pressure P_s is 25bar, the primary pressure P_p^* at a steady state is obtained as $P_p^*=$ 10bar (point A) from the line of $di/dt=0$. If we carry out the upshift from A by increasing the primary pressure to the line pressure $P_s=25$bar, the maximum upshift speed obtainable is determined as $di/dt=-1.1$ (point B). From the shift speed map, it is obvious to achieve a faster shift speed by increasing the line pressure. For example, if we increase the line pressure up to 35bar (point C), the shift speed obtainable becomes $di/dt=-1.6$.

The shift speed map for the downshift case is shown on Fig. 2. The shift speed map is constructed when the downshift is carried out from the highest gear ratio, $i=0.49$ while the primary speed is maintained at $\omega_p=2000$rpm. At the highest gear ratio, the primary pressure P_p^* at a steady state maintains 25bars which is equal to

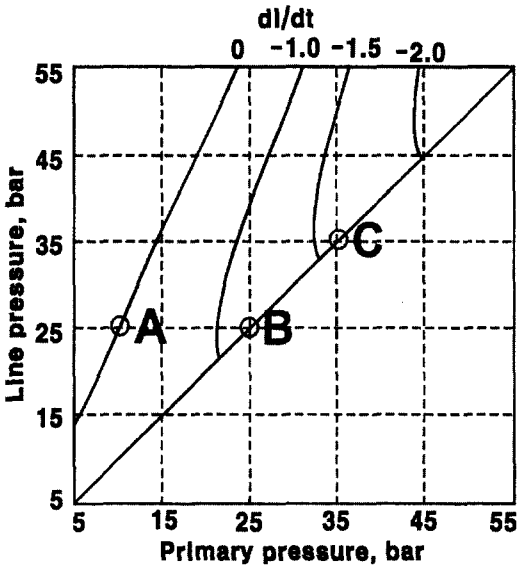

Fig. 1 Shift speed map toward high speed ratio from $i=2.48$

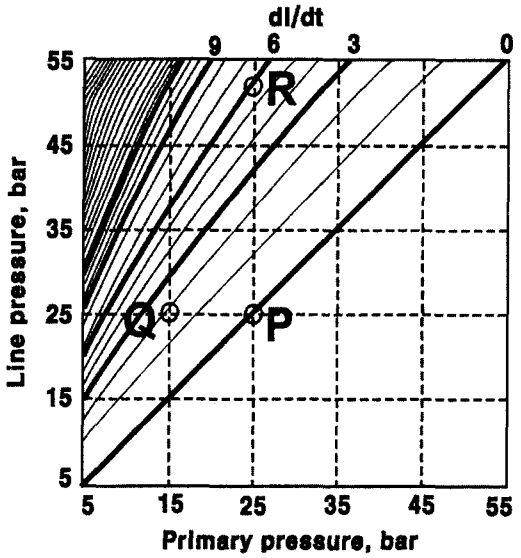

Fig. 2 Shift speed map toward low speed ratio from $i=0.49$

the line pressure (point P). The downshift can be performed by reducing the primary pressure or by increasing the line pressure. For instance, if we decrease P_p to 15bars (point Q), the shift speed $di/dt=2.0$ can be achieved. When a faster shift speed, for example, $di/dt=6.0$ is desired, it is possible to achieve it by the following two ways; one is to reduce the primary pressure down to $P_p=7$bars. However, an excessive reduction in the primary pressure may cause a belt slippage. The other way is to increase the line pressure up to 52bars (point R).

The shift speed map can be constructed similarly for various speed ratios for the upshift and the downshift case and a faster shift speed can be achieved by increasing the line pressure based on the shift speed map. It is seen from Eq. (2) and Fig. 1~Fig. 2 that the shift speed of CVT is a function of the line pressure as well as the primary speed. Therefore, it is possible to obtain a faster shift speed by increasing the line pressure.

In order to implement Eq. (2), the target shift speed needs to be defined. In this study, the target shift speed $di/dt\,|_{target}$ is defined as:

$$\left.\frac{di}{dt}\right|_{target}=\frac{id-i}{\Delta t} \tag{3}$$

where i_d is the desired ratio, i is the actual ratio and Δt is the sampling time.

Once the target shift speed is determined, the target line pressure $P_{s\,target}$ can be obtained from Eq. (2) for a given target speed, $di/dt\,|_{target}$ as follows,

$$P_{s\,target}=\frac{\left.\frac{di}{dt}\right|_{target}}{\alpha(i)\cdot\omega_p\left(1-\frac{P_p^*}{P_p}\right)} \tag{4}$$

In this way, the shift speed control is performed. It is expected that a faster shift speed is able to provide an improved engine operation on the OOL for the minimum fuel consumption. Therefore, an improved fuel economy can be obtained by increasing the shift speed. However, the faster shift speed, in other words, the increased line pressure causes an additional hydraulic power loss. The hydraulic loss is represented as,

$$P_{hydraulic\,loss}=P_sQ \tag{5}$$

It is seen from Eq. (5) that an excessive line pressure may results in a worse fuel economy. Therefore, considering the hydraulic power loss which results from the increased line pressure, the shift speed control algorithm is applied only when the following conditions are met,

$$i_d-i<-\gamma \text{ and } \frac{d\theta}{dt}<q \tag{6}$$

where θ is the accelerator pedal opening, γ and q are the constant. Equation (6) shows that the shift speed control algorithm is applied when the difference between the desired ratio and the actual ratio is less than $-\gamma$ and the accelerator pedal speed is not high. The minus sign means that increasing the shift speed is performed only when the upshift is carried out. In other words, the shift speed improvement is pursued only for the upshift in a moderate driving in which the shift speed and the accelerator pedal speed are relatively slow. When a fast downshift is required such as in the kickdown maneuver, the maximum shift speed that can be obtainable is applied. Figure 3 shows a block diagram of the shift speed control algorithm.

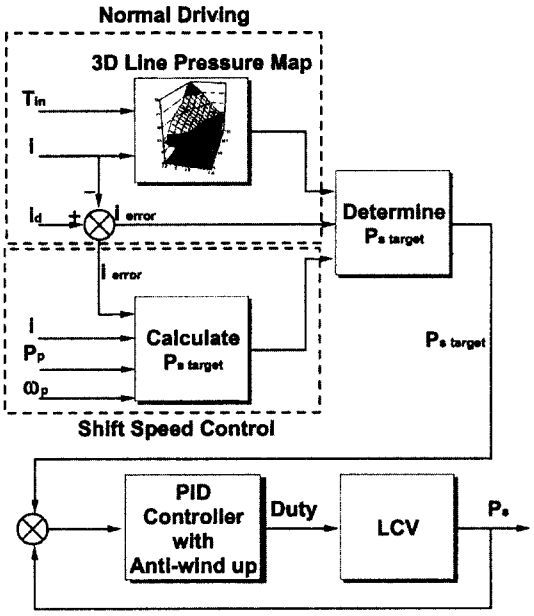

Fig. 3 Block diagram of shift speed control algorithm

3. Control Valve Modeling

3.1 Line pressure control valve

In Fig. 4, schematic diagram of an electronically controlled CVT used in this study is shown. The line pressure is regulated by the line pressure control valve (LCV), which is operated by a variable force solenoid (VFS) type line pressure control solenoid valve (LCSV). The LCSV generates a control pressure P_c which is applied to the land #1 of the LCV spool. If the input duty decreases, P_c increases and the spool moves to the right side to close the exhaust port, which results in the increased line pressure. If the input duty increases, P_c decreases and the decreased line pressure is obtained. So, the line pressure control is achieved by the LCSV duty control. The ratio control valve (RCV) is also operated by the VFS type ratio control solenoid valve (RCSV). If the input duty increases, the control pressure applied to the land #2 of the RCV spool decreases, so the spool moves to the left side. This causes the exhaust port to open, thus the primary pressure decreases and the belt pitch radius decreases, which results in the downshift of the CVT ratio.

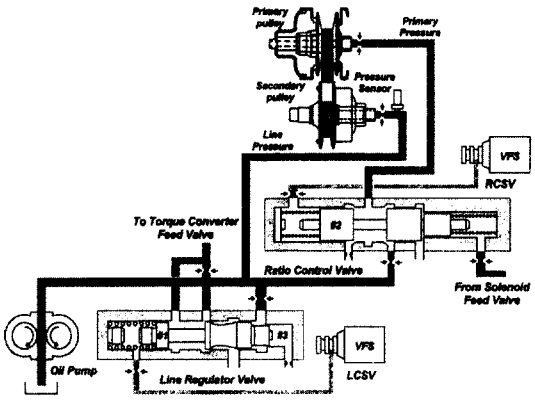

Fig. 4 Schematic diagram of an electronic controlled CVT

The upshift can be obtained by decreasing the duty ratio of the RCSV.

In this study, considering the ineffective duty region of the VFS valves and the oil pump flow characteristics, the LCV is modeled as the following second order system.

$$P_s=\frac{K_1(\omega_{pump})\,\omega_n^2}{s^2+2\zeta\omega_n s+\omega_n^2}duty+K_2(\omega_{pump}) \quad (7)$$

where K_1 and K_2 are the coefficients depending on the oil pump speed, ζ is the damping coefficient, ω_n is the natural frequency. K_1, K_2, ζ and ω_n are determined from the experiments.

3.2 Ratio control valve

In order to obtain the dynamic model of the RCV, not only the ineffective duty region of the VFS but also the oil flow to and from the actuator during the shift need to be considered. In Fig. 5, the RCV dynamic model is shown. As shown in Fig. 5, the RCSV is modeled as a second order system which produces the RCV spool displacement for a given duty input. The RCV inlet and exhaust port area are determined from the spool displacement x. Consequently, the RCV is modeled as an orifice area generator. State space equation of the primary pressure is represented as,

$$P_p=\frac{\beta}{V_p+A_pX_{pp}}\left(Q_{pin}-Q_{pout}-A_p\frac{dX_{pp}}{dt}\right) \quad (8)$$

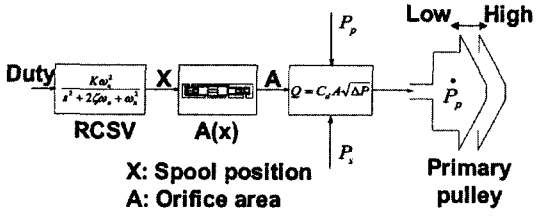

Fig. 5 Dynamic model of RCV

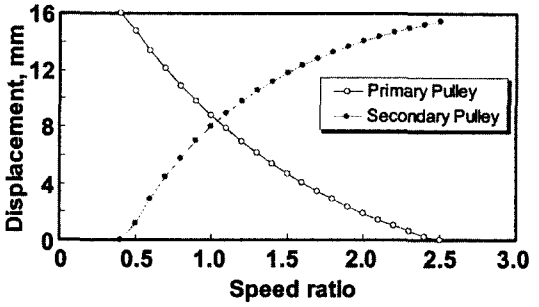

Fig. 6 Movable pulley displacement vs. speed ratio

where Q_{pin} and Q_{pout} are the oil flow to and from the primary actuator respectively. The last term in Eq. (8) represents the oil flow change occurred during the shift. dX_{pp}/dt is the movable flange speed. dX_{pp}/dt can be obtained from the shift speed and the CVT geometry as,

$$\frac{dX_{pp}}{dt}=\frac{di}{dt}\cdot\frac{dX_{pp}}{di} \tag{9}$$

where dX_{pp}/di is the gradient of the speed ratio with respect to the flange displacement and depends on the CVT geometry. Figure 6 shows a relationship between the CVT ratio i and the movable flange displacement X for the primary and the secondary pulley. The gradient dX_{pp}/di can be obtained from Fig. 6 and the shift dynamics shown on Eq. (1).

4. Vehicle Model

Dynamic model of the vehicle and the engine are represented by the following equations,

$$\dot{V}=\frac{F_d-F_L-F_b-\dfrac{\eta_f\eta_t\eta_g iN_f^2\dfrac{di}{dt}J_{eq}}{R_t^2}}{M+\dfrac{\eta_f\eta_t\eta_g i^2N_f^2}{R_t^2J_{eq}}} \tag{10}$$

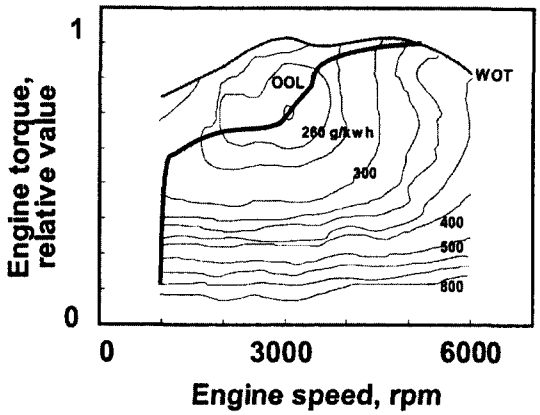

Fig. 7 Engine map and OOL

$$\dot{\omega}_e=\frac{1}{J_e}(T_e-T_c-T_{loss}) \tag{11}$$

where F is the force, T is the torque. Subscript d, L, b, e, c and loss represent drive, road load, brake, engine, clutch and loss respectively. N_f is the final gear ratio, M is the vehicle mass, J_{eq} is the equivalent inertia, R_t is the tire radius, η_f, η_t and η_g are the efficiency of the final reduction gear, CVT and the gear train. A wet type multi-disc clutch is used as the starting element.

Figure 7 shows the engine map and the OOL of a 1.6L DOHC engine used in the simulation.

5. Simulation Results and Discussion

Simulations are carried out to estimate the performance of the shift speed control algorithm. Simulation results with the shift speed control algorithm (b) are compared with those without the algorithm (a) in Fig. 8. Simulation results in Fig. 8 show the response of the first 400 seconds for federal urban driving schedule(FUDS). In performing the simulation, a safety factor of 1.3 is applied in calculation of the line pressure for both (a) and (b) even when the shift speed control algorithm is not required. In Fig. 8 ①, the actual vehicle velocity V is compared with the desired velocity V_d. It is seen that V follows V_d closely for both (a) and (b). The actual CVT ratio i also follows the desired ratio i_d (②). The line pressure with the shift speed control algorithm ((b)-③) shows higher values than the

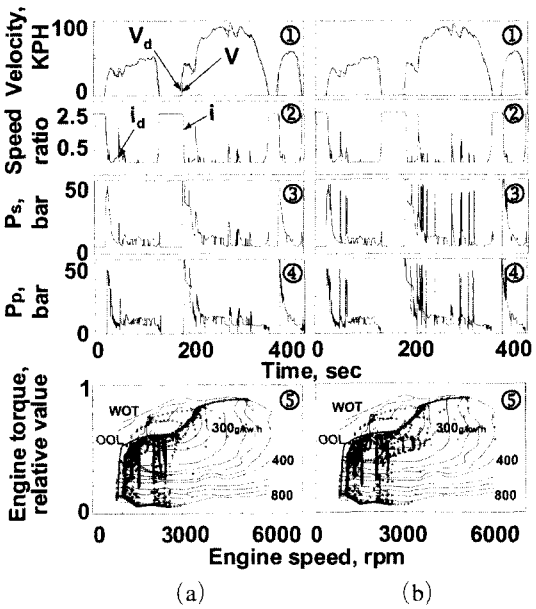

Fig. 8 Comparison of simulation results for shift speed control algorithm not applied (a) and applied (b)

pressures without the algorithm ((a)-③) when the upshift is carried out according to the algorithm, Eq. (2)～Eq. (4). The primary pressure ④ changes to generate the desired speed ratio and also shows higher values than the pressures without the algorithm. The engine operation trajectory of (a) looks almost similar with that of (b). However, it is noted that the engine operation of (b) is performed more closely on the OOL in the speed range of 2500～3000rpm.

In Fig. 9 and Fig. 10, closer look of the CVT ratio and the engine trajectory are shown for 20～60seconds of FUDS. As shown in "A" in Fig. 9, the CVT ratio response shows time delay when the speed ratio changes from the lowest gear ratio. This time delay is due to the inherent characteristics of the CVT, such as a time to fill up the empty volume of the actuator when the upshift begins from the lowest gear ratio. It is noted from "B" that a faster shift (b) is obtained according to the shift speed control algorithm when the upshift is required. The engine operation trajectories for 20～60 seconds are compared in Fig. 10. It is seen that the engine operation by the shift speed control algorithm is performed

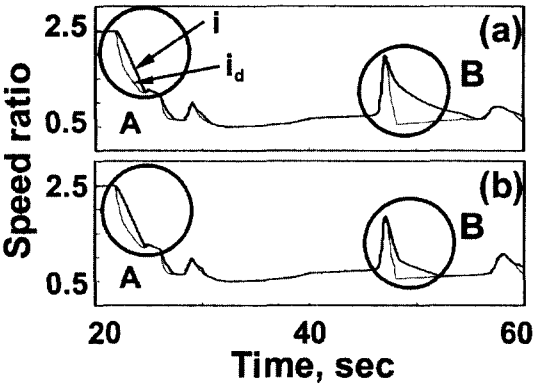

Fig. 9 Comparison of speed ratio response

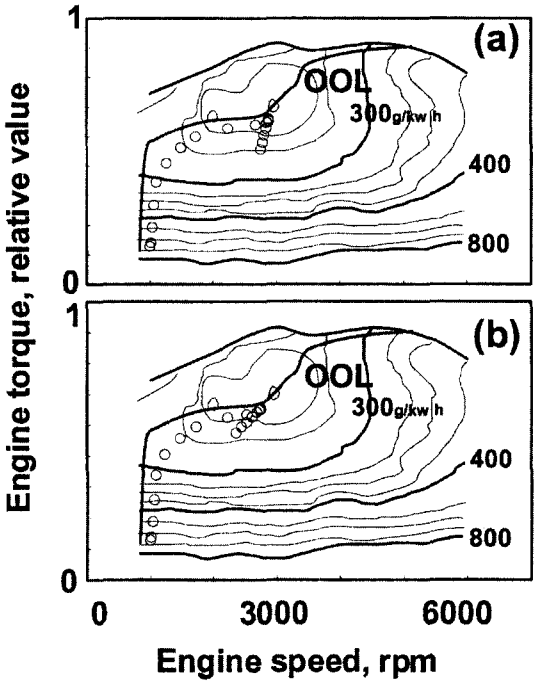

Fig. 10 Comparison of engine trajectory

more closely on the OOL.

Figure 11 shows the effect of parameter γ in Eq. (6) on the vehicle performance. As shown in Fig. 11, as γ increases, the hydraulic power loss decreases since the driving time where the increased line pressure is required by the shift speed control algorithm decreases. However, comparing the hydraulic power loss with the shift speed control algorithm with that of the conventional electronic control CVT, the hydraulic loss adopting the shift speed control algorithm is higher than that of the

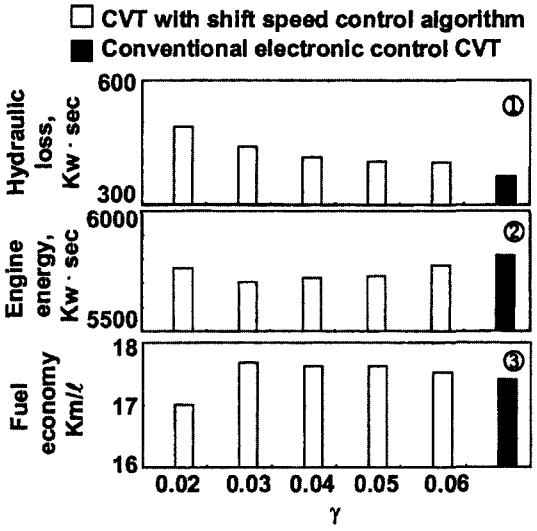

Fig. 11 Comparison of simulation results for various γ

conventional CVT as expected. The engine energy consumed during FUDS is shown on Fig. 11-②. It is noted that the engine energy for the shift speed control algorithm is smaller than that of the conventional electronically controlled CVT in spite of the increased hydraulic power loss, which is owing to the improved engine operation on the OOL by the faster shift speed. The lowest engine energy is obtained at $\gamma=0.3$ for the engine used in this study. Correspondingly, the best fuel economy can be achieved at $\gamma=0.3$. Comparing the fuel economy, it is seen that 2% improvement can be obtained by the shift speed control algorithm.

6. Conclusion

(1) An algorithm to improve the engine operation on the optimal operating line is suggested by controlling the shift speed for a metal belt CVT. In order to obtain a faster shift speed, algorithms to calculate the line pressure to achieve the target shift speed is suggested and a criterion for the shift speed range is proposed by considering the additional hydraulic loss due to the increased line pressure.

(2) Performance simulation of the CVT vehicle is carried out by using the dynamic models of the CVT shift dynamics, line pressure/ratio control valve, powertrain and vehicle dynamics. It is found that the fuel economy can be improved about 2% for FUDS by the shift speed control algorithm in spite of the additional hydraulic loss.

References

Ide, T., Uchiyama, H. and Kataoka, R., 1996, "Experimental Investigation on Shift Speed Characteristics of a Metal V-Belt CVT," *Proceedings of the International Congress on Continuously Variable Power Transmission*, pp. 59~64.

Kim, T. and Kim, H., 2000, "Integrated Engine-CVT Control Considering Powertrain Response Lag in Acceleration," *KSME International Journal*, Vol. 14, No. 7, pp. 764~772.

Lee, H. and Kim, H., 2001, "Shift Speed Improvement of a Metal-Belt CVT," *KSME International Journal*, Vol. 15, No. 12, pp. 1623~1629.

Maaike van der Laan, 1999, "Model-Based Variator Control Applied to a Belt Type CVT," *Proceedings of the International Congress on Continuously Variable Power Transmission*, pp. 105~110.

Serrarens, A. F. A. and Veldpaus, F. E., 1999, "Powrtrain Control of a Flywheel Assisted Driveline with CVT," *Proceedings of the International Congress on Continuously Variable Power Transmission*, pp. 225~230.

Vroemen, B. G., Serrarens, A. F. A. and Veldpaus, F. E., 2001, "Hierarchical Control of the Zero Inertia Powertrain," *JSAE Review*, Vol. 22, pp. 519~526.

Vroemen, B. G. and Veldpaus, F. E., 1999, "Hydraulic Circuit Design for CVT Control," *Proceedings of the International Congress on Continuously Variable Power Transmission*, pp. 111~116.

Vroemen, B. G., 2001, "Component Control for The Zero Inertia Powertrain," Ph. D dissertation, Technische Universiteit Eindhoven, Netherlands.